BIOIMPEDANCE

As an introduction to electrical impedance and conductance in biology, a review of the relevant terminology is given and the scope of the discipline is presented. The area of bioimpedance is broad, including, for example, impedance cardiography, electrode impedance, impedance spectroscopy, intraluminal conductance, and impedance tomography. The field of bioimpedance deals with the electrical conduction properties of biological materials as a response to the injection of current. It has been known for more than two centuries that biological structures display the phenomenon of electrical conduction. Later, it was found that the precise electrical properties of tissues depend on their cellular composition and their coupling. These characteristics imply that the voltage changes at a particular site may provide valuable information regarding the biological materials and processes concerned.

However, to date, our understanding of the electrical impedance of biological tissues and their changes, as far as they are associated with physiological activity, is still limited. This article discusses the application of electrical impedance in medicine. Briefly, bioimpedance can be used to quantitate extracellular fluid, to assess volume changes, and as an imaging tool similar to ultrasonography. Reviews can be found in (1–3), and (4).

In order to meet the requirements of specific applications, electrodes for delivering or recording electrical potentials in biological structures appear in a variety of materials, sizes, and shapes. The interface between electrode and tissue has been studied extensively (5, 6).

IMPEDANCE CARDIOGRAPHY

Impedance cardiography (ICG) is the noninvasive measurement of physiologically and clinically relevant parameters of the heart and circulation, based on electrical impedance measurements of the thorax during the cardiac cycle. Recent reviews have been presented by (7) and (8). The technique uses a low-current (0.5 mA to 4 mA), high-frequency (50 kHz to 100 kHz), alternating current across the thorax, not perceivable to the subject. The resulting impedance changes associated with the cardiac cycle (impedance decreases by about 0.2 Ω from diastole to systole) provide information on stroke volume, cardiac output, pulmonary capillary wedge pressure (9), and systolic time intervals (by calculating the first time derivative of the impedance waveform). In 1969, (10) suggested an index of cardiac function based on particular calculations applied to the impedance tracing. This so-called Heather index was shown to correlate with the severity of cardiac pathology (7).

Among other techniques to measure cardiac size (e.g., X ray, ultrasound, magnetic resonance imaging), external impedance cardiography has the advantages of being noninvasive, requiring only relatively low-cost equipment, and permitting continuous monitoring of signals originating from the beating heart, even during exercise (11). Major shortcomings result from the fact that a sound physical model and a comprehensive theory still need to be developed. (12, 13), and (14) were among the first researchers to study the feasibility of the method. Chest impedance is determined by the relatively constant electrical conduction properties of all tissues concerned, plus a modulated component caused by the combination of respiration, thoracic dimensional changes, and a cardiovascualr size-related factor. The latter component is due to cyclic changes of size (i.e., the geometry changes with contraction) of the four compartments of the heart and the major blood vessels, as well as to the periodic alignment and deformation of the erythrocytes in the flow. Ejection of blood from the heart distends the walls of the arteries, thus increasing their blood volume and resulting in an impedance decrease, besides a decrease of lung resistivity owing to blood perfusion. During relaxation of the cardiac ventricles, blood in the systemic circulation travels downstream, causing a reduction of the arterial diameter while the erythrocytes lose their orientation owing to the lower velocity, all leading to an increase of the thoracic impedance. Using suitable filtering techniques, it turns out that the contributions derived from breathing and locomotion can be eliminated. Obviously, respiratory components are simply removed if patients are instructed to temporarily hold their breath, but in animals this approach would not be feasible. Various filtering procedures have been developed, including Fourier linear combiner (*FLC*) and event-related transversal types. A major problem is that many physiological signals are quasiperiodic; that is, they have a mean period with a small random variation around this mean at each interval. (15) introduced a scaling factor to enhance flexibility when choosing filter parameters in the FLC approach. They successfully applied their method to ICG-derived stroke volume (*SV*) in a volunteer during exercise. Alternatively, one may apply an ensemble averaging technique to 20 beats, thus eliminating respiratory influences (16). The number and position of the electrodes employed may vary depending on the specific purpose of the study or the particular geometrical model assumed. Basically, a four-electrode (tetrapolar) arrangement is employed: two current injecting electrodes form the outer pair, and the inner two are the sensing electrodes. This setup overcomes not only impedance problems related to electrode polarization but also the relatively high skin impedance. A typical configuration for ICG is illustrated in Fig. 1.

The amount of blood pumped per minute by one side of the heart is termed cardiac output (CO) and equals the product of heart rate (HR) and SV. In ICG it is the passage of blood in the major arterial vessel (called the aorta) during the ejection phase of the ventricle that mainly determines the changes in electrical impedance. In contrast, the electrocardiogram (ECG) is a recording of the electrical wavefront as it spreads over the cardiac tissues, and this signal provides no information on the amount of blood pumped nor does it give any insight into the size of the ventricle or the strength of contraction. Therefore it is important to emphasize that the actual (internal) source of electricity in the heart, namely, the action potentials that cause a periodic voltage change on the order of 100 mV over the cell membranes of the heart, are unrelated to the electrical impedance variations resulting from the external stimulation electrodes and as recorded by the sensing

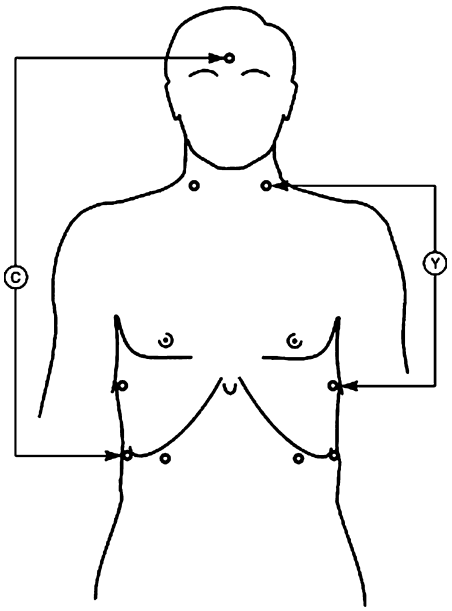

Figure 1. Electrode configuration for thoracic impedance cardiography: V, the voltage recording electrodes on the lateral base of the neck and another pair on the chest at the level of the xyphoid; C, constant current-injecting electrodes on forehead and at abdomen placed 15 cm caudally from the voltage electrodes.

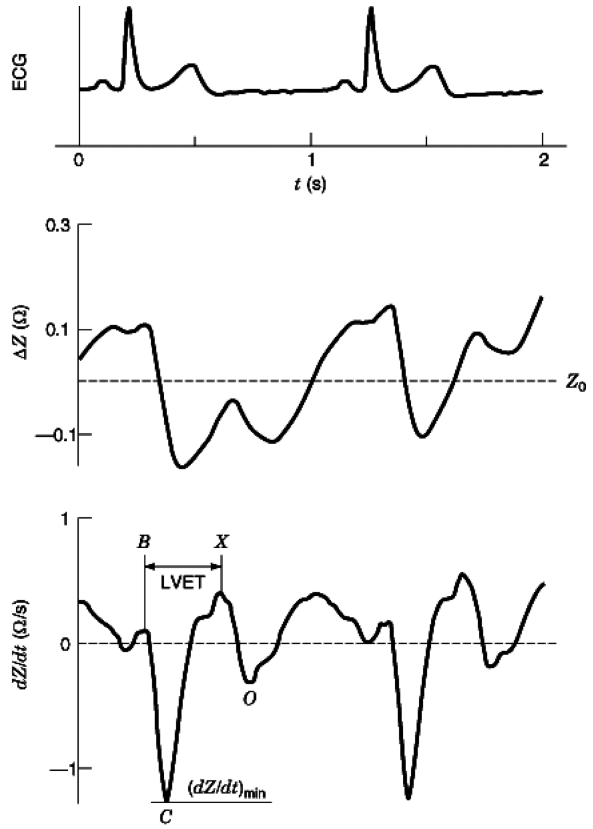

Figure 2. Left ventricular (LV) volume as obtained by intraventricular impedance catheter in the open-chest dog. Also shown is the flow in the aorta resulting from these volume changes during an episode of irregular heart rhythm. (From Ref. (35) with permission.)

electrodes. It may be concluded that the ECG and the thoracic impedance signal provide complementary information on the activity of the heart: the ECG on the internally generated electricity, and the thoracic impedance on the hemodynamic changes owing to the mechanical action of the heart.

The electrical impedance signal is obtained from a special arrangement of disposable spot or band electrodes placed on the skin of the head, neck, and chest. A set of current-injecting electrodes is driven by a constant sinusoidal current of less than 1 mA root mean square at a frequency ranging from 50 kHz to 100 kHz, while another set of electrodes senses the resulting voltage from which the impedance signal is calculated. The peripheral ECG is usually recorded from the limb leads (Fig. 2).

Thoracic impedance (Z) has a baseline component Z_0 and a time-variable component (dZ). Z_0 depends on posture, tissue composition, and the volume of fluids within the chest. Cardiac edema causes a decrease of the value for Z_0 (17). In noncardiac edema (e.g., in the adult respiratory distress syndrome), Z_0 can increase or decrease owing to capillary leakage of proteins (18). The component dZ corresponds to the volume change in the thoracic aorta during the cardiac cycle. The maximum value of the time derivative of ΔZ is proportional to the peak ascending aortic blood flow. (13) developed a formula to derive SV (in mL) from the thoracic ICG:

$$SV = \rho T_{\mathrm{et}} (L/Z_0)^2 (dZ/dt)_{\mathrm{min}}$$

where ρ is the specific resistivity of blood (about 135 Ω·cm and 150 Ω·cm for women and men, respectively), T_{et} the duration of the ejection period (s), L the distance between both recording electrodes (cm), and Z_0 the baseline component of the thoracic impedance (Ω). This approach has been widely applied, sometimes after modification of the expression to account for body build. Underlying assumptions for Kubicek's equation and subsequent modifications are that the tissues are modeled as a homogeneous electrical conductor with the shape of a cylinder or truncated cone, and that the impedance variations observed in synchrony with the heartbeat exclusively reflect the time-varying volumetric changes of the cardiovascular system in the specific model considered. For the cylinder model, the length is related to the height of the chest, while the cross-sectional area reflects the thoracic circumference; the values of these parameters are obviously characteristic for each individual at a given time. (19) determined the inaccuracy of Kubicek's one-cylinder model, or more generally of any geometrical model with a uniform cross section, both in a theoretical study and using *in vivo* experiments. The results indicate that the one-cylinder model is not valid and must be replaced by a model with two serially placed cylinders, which appropriately exhibit a length-dependent behavior corresponding to differences in body height and mass. It was concluded that corrections for the Kubicek equation are required, along with the incorporation of a two-cylinder model. Interestingly, (20) found for the truncated cone model no gender effect on SV when normalized for body surface, because the differences in the component

Z_0 were counterbalanced by changes in dZ. However, both in females and in males they documented a decline of normalized SV with age (range 20 years to 69 years).

As an extension of the routine approach to estimating SV by thoracic impedance and using the Kubicek equation, (9) also found a high correlation with the clinically important pulmonary capillary wedge pressure (PCWP), which corresponds to left atrial pressure and thus reflects left ventricular filling. They also compared the noninvasively obtained SV with values determined by thermodilution. The study population consisted of 24 patients with cardiac problems, including coronary artery disease and various types of valvular defects. The PCWP as determined with a pulmonary artery catheter correlated ($r = 0.92, p < .0001$) with the ratio obtained by dividing the amplitude of the ICG during diastole (the O-wave) by the maximum value during systole. It was hypothesized that this ratio reflects efficiency of the left ventricle (LV) because the O-wave corresponds with preload, whereas the peak of dZ/dt is related to afterload. A comparison between the two methods (i.e., impedance versus thermodilution) to estimate SV was less encouraging ($r = 0.69, p < .05$), particularly for patients with valvular disease. As an extension, (21) assessed right ventricular diastolic function in patients with chronic obstructive pulmonary disease by means of region of interest analysis applied to electrical impedance tomography, as will be described later.

Of crucial importance, of course, is a quantitative validation of the thoracic impedance method, preferably using a gold standard for the determination of SV. Unfortunately, an ideal reference technique does not exist, and therefore researchers often rely on methods that are feasible and minimally traumatic. For example, (22) recently performed a comparison of hemodynamic parameters derived from transthoracic electrical bioimpedance with those obtained by thermodilution and ventricular angiography. These investigators studied 24 human patients with coronary artery disease while employing the three independent methods and concluded that impedance cardiography should not replace invasive hemodynamic monitoring. However, an accompanying editorial moderated this pessimistic conclusion by pointing to the expected impact from emerging noninvasive echocardiographic Doppler technology.

As mentioned before, the physical size and shape of an individual are related to the dimensions considered in any geometrical model such as the cylinder or the truncated cone. For a given adult these values may be expected not to change very much, unless a disproportionate dimensional change occurs within a relatively short time frame. In pregnancy, for example, maternal blood volume increases by about 40%, while CO reportedly rises by some one-third within nine months. Therefore, in longitudinal studies involving pregnant women, certain precautions may be indicated. (23) addressed the question of whether thoracic electrical bioimpedance is suitable for monitoring SV during pregnancy. It was demonstrated that the Kubicek formula for SV needs to be modified by a multiplication factor, which for each woman is to be determined at the beginning of the pregnancy period. Subsequently, (24) explored the possibility of relating CO to body surface area in women during the course of their pregnancy. Based on the poor correlations found for both impedance and Doppler echocardiographic data, the authors concluded that normalized CO does not offer any additional information relevant for comparative evaluations during pregnancy and may even be misleading.

The availability of ICG as a measurement technique that is noninvasive and permits continuous registration evidently opens the way to investigations of circadian effects. (25) took advange of these properties of ICG and studied sleep and circadian influences on the cardiac autonomic nervous system activity. They found that parasympathetic activity (derived from respiratory sinus arrhythmia observed in the ECG) is mostly influenced by the circadian system, whereas sympathetic nervous system activity (assessed with the pre-ejection period of the impedance signal) is predominantly affected by the sleep system.

Unfortunately, there exists no "gold standard" for cardiac size determination, because most techniques require barely verified assumptions concerning anatomical geometry. A similar shortcoming also applies to SV, which refers to the difference between diastolic and systolic volumes. Another approach would be to compare SV as measured in the aorta using a flow probe with the ICG signal; such as experiment will be feasible in the chronically instrumented animal and therefore deserves due attention.

Two types of problems related to application of the ICG will be discussed. First is the type of electrodes employed, that is, band (or tape type, consisting of a 6 mm conductive foil strip) versus spot (or regional) electrodes. The band signal is made up of different signals from various regions and may reflect changes in SV (rather than the absolute value), whereas spot electrodes may be important in measuring regional physiological activities of the central circulation (11, 26). Also, the anatomical position of the electrode and movement can cause large artifacts that may override the signal of primary interest (27). Second, the commonly made assumption that aortic distension during the ventricular ejection phase is the predominant component is not justified, because concomitant changes of lung resistivity, ventricular contraction, and other factors may interfere with comparable magnitude (26, 28). Obviously, the current limitations preclude wide clinical acceptance and certainly require further measurement refinements of the ICG method, but recently progress has been made in this field (19–29).

CONDUCTANCE MEASUREMENTS

Besides the method of measuring external impedance changes caused by the mechanical activity of the heart, it is also technically possible to record conductance changes within the lumen of each cardiac compartment. Since the beginning of this century, scattered reports were published about the recording of cardiac volume changes derived from impedance measurements by placing electrodes on the heart. (30) placed electrodes on the inside of the ventricular wall, but practical problems concerning the electrodes delayed progress in this field. In 1961 the Brazilian dentist A. Mello-Sobrinho started experiments with a

bipolar arrangement, where electrodes mounted on pointed rods were passed through the myocardium and sutured to the apex and base of the left ventricle of a dog; he succeeded in producing intraventricular pressure–impedance loops (31). Tremendous advances were made when multiple electrodes were mounted on a catheter, which can be positioned along the long axis of the ventricle. Because such a catheter usually is introduced via a peripheral artery, there is no longer a need to open the chest in order to carry out the internal impedance measurements. The catheter technique has been pioneered by the research group of Baan at Leiden University (32–35) with applications in both animals and humans. Obviously, this approach implies an invasive procedure (called cardiac catheterization) but has the advantage that geometrical variation associated with the cardiac cycle can be measured at a segmental level. The theoretical background of the impedance catheter, a term that was coined in the early phases, and its application to cardiac volumetry have been described by (32). In their model, the left ventricular cavity and the myocardial wall are represented by two confocal spheroids. The wall is included because the impedance signal is permanently affected by a certain amount of current that leaks into the ventricular wall and the surrounding extracardiac tissues. This offset component, the so-called parallel conductance (34), can be determined by a relatively simple intervention, the injection of chglucose or hypertonic saline (35). A new technique, using dual-frequency excitation, eliminates the need for such an intervention and offers the additional advantage of providing continuous information on this offset component without physiological interference (36). The method exploits the fact that muscle and blood exhibit different conductivities depending on the frequency employed. Muscle tissue is more conductive at frequencies above 12 kHz when the current is applied in a direction normal to the fiber orientation (37), while the conductivity of blood is essentially constant within the range of 2 kHz to 100 kHz. While this technique elegantly solves problems inherent in parallel conductance for a particular heart under investigation, the question whether parallel conductance is independent of left ventricular size remains controversial. (38) used the conductance catheter for the measurement of left ventricular volume in the intact dog to study whether parallel conductance is independent of left ventricular size, that is, if it is constant throughout the cardiac cycle. In contrast to the findings of other investigators, these authors concluded that parallel conductance varies between animals, but within any given animal parallel conductance does not decrease with left ventricular size, but rather remains constant.

APPLICATIONS OF CONDUCTANCE METHODS IN VARIOUS SPECIES

While the dog is historically employed as a standard animal in cardiovascular research, today we witness conductance applications in a variety of species. Regarding the canine heart an example is given in Fig. 3.

(39) applied the conductance catheter to the left ventricle of newborn lambs and demonstrated a clear interaction between afterload and contractility. Preload and afterload were varied by inflating a balloon catheter positioned in the posterior vena cava and the thoracic aorta, respectively. In these anesthetized neonates the authors found evidence of homeometric autoregulation, enabling the heart to maintain SV at different levels of afterload. Both (40) and (41) developed a microconductance device (8 mm $\times$ 2 mm $\times$ 0.5 mm) and a 3F catheter, respectively, so as to accommodate the standard number of six to eight electrodes of a probe suitable for use in the rat heart.

As a variant to the dilution technique, (42) measured CO in small laboratory animals using recordings of blood conductivity. A 5% glucose solution was injected as a bolus via the femoral vein of mice and rats. The changes of blood conductivity resulting from this perturbation were recorded by an intra-aortic probe with platinum electrode combined with another one positioned within the rectum, and this signal was used to calculate CO. Other investigators previously applied the method in dogs, and for these small animals an excellent correlation ($r = 0.97, p < .001$) with the classical type of the indicator dilution method was observed.

(43) were the first investigators to simultaneously measure left ventricular (LV) pressure (P) and volume (V) in the horse. Thus far, the conductance catheter was applied to obtain V for clinical evaluations in human patients, and also for experimental investigations in animals. While there is a tendency to miniaturize catheters and study small species such as rats, larger animals like the horse have not been evaluated with this instrument. They investigated the P–V relationship in three anesthetized ventilated horses, with body mass ranging from 250 kg to 600 kg. Introduced via the carotid artery, they employed a 7F Millar P-catheter and a large-size conductance catheter (outer electrodes 20 cm apart, with four equidistant sensing electrodes) built at their institution. Respiration in terms of chest wall excursion was externally recorded using a mercury-in-silastic gauge placed around the chest. Reliable measurements were obtained including LV volume at segmental levels, while P–V loops could be constructed. An example is given in Fig. 4. In these preliminary experiments calibration procedures were not yet carried out, and therefore V data are presented as arbitrary units (A.U.). Yet, the relative values and the time relationships with left ventricular pressure and the pneumogram are still applicable and informative.

This pilot study demonstrates the feasibility of performing P and V measurements in the adult equine model. The slow heart rate and the large LV dimensions in the horse permit detailed analysis of the hemodynamic consequences of asynchronous contraction patterns, while fully employing the potential of the conductance catheter to measure LV contraction at segmental levels.

AORTIC CROSS-SECTIONAL AREA MEASUREMENT

Arterial transverse dimensions change with the cardiac cycle, periodically resulting in extension during the ejection phase followed by relaxation during the diastolic phase of the ventricle. These varying dimensions can potentially be

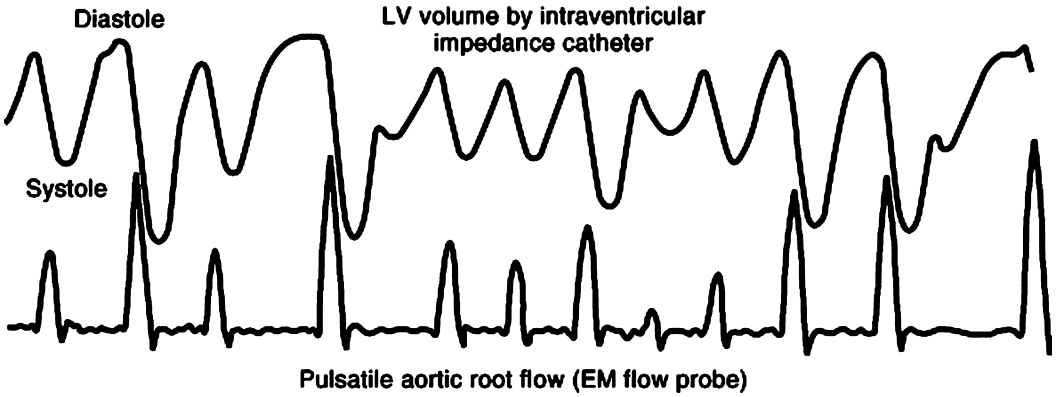

Figure 3. Left ventricular pressure–volume loops recorded in the anesthetized horse. (From Ref. (43), with permission.)

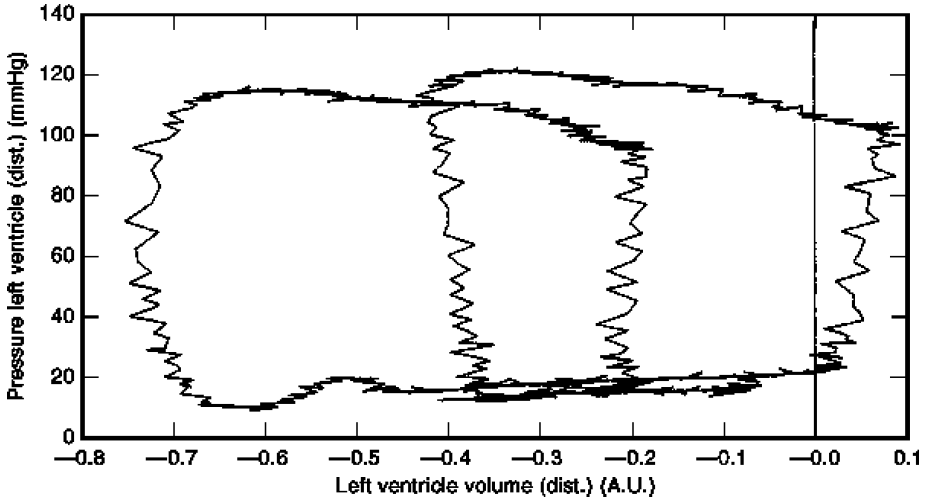

Figure 4. Variations of left ventricular and atrial cross-sectional area in the magnetic resonance imaging (MRI) and the electrical impedance tomography (EIT) images made with the person in the supine position. (From Ref. (29), with permission.)

measured using the electrical impedance technique with electrodes positioned within the lumen of the blood vessel. Actually, various methods have been developed to assess continuously the aortic cross-sectional area (CSA), including the intravascular ultrasound (*IVUS*) method. (44) reported in 1979 the feasibility of the impedance method for determining CSA. They noted that movement of the catheter toward the vessel wall consisted of a calculated error (maximally 7%), which is considered to be of minor importance. (45) refined the method and compared the findings with results obtained from IVUS (range 35 mm^2 to 70 mm^2), yielding a correlation coefficient of 0.97 for 53 data points collected from experiments in five piglets.

IMPEDANCE PNEUMOGRAPHY

The plethysmographic technique employs a device that records respiratory excursions from movements of the chest surface on the basis of electrical impedance variations. Originally, the method was applied to the detection of apnea (i.e., suspension of respiration) in newborns, and for tracking changes in intrathoracic fluid accumulation (46). Other approaches such as the spirometer and the pneumotachometer have the disadvantage that they require insertion into the airway. The four-electrode arrangement uses an electrode on each wrist, to which a constant 10 kHz low-intensity current is applied, and an electrode on each arm to record the impedance changes. As an alternative, one may measure variations in electrical resistance of a mercury-in-silastic-rubber gauge mounted around the thorax. Using a Wheatstone bridge it is rather easy to follow the periodic alterations caused by respiratory movements of the chest (Fig. 5). For further details see the paper by (47).

APNEA MONITORING

Sleep apnea is defined as temporary interruption of airflow to the lungs during the sleeping period and lasting for more than ten seconds. This abnormality usually results either from upper airway collapse (obstructive type) or, in 10% of the cases, from the absence of diaphragmatic contraction due to the lack of neural input (the central type) from the brain, although mixed types do occur. Such conditions are usually associated with loud snoring, while general symptoms and signs include fatigue, hypersomnolence during

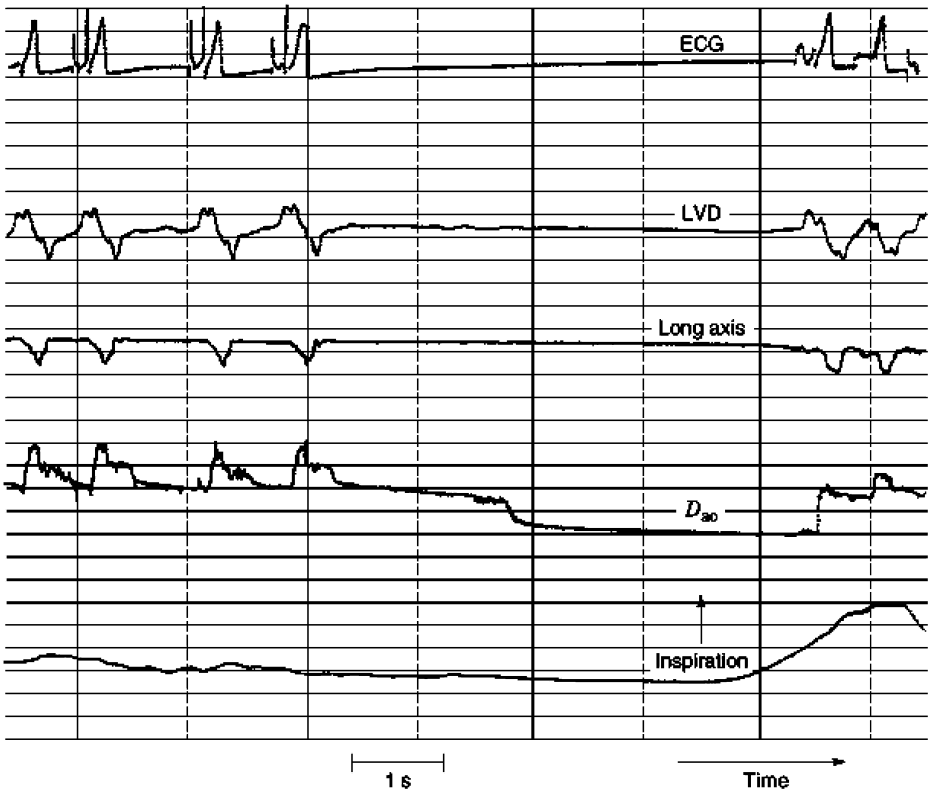

Figure 5. Cole–Cole diagram for an impedance with a single time constant.

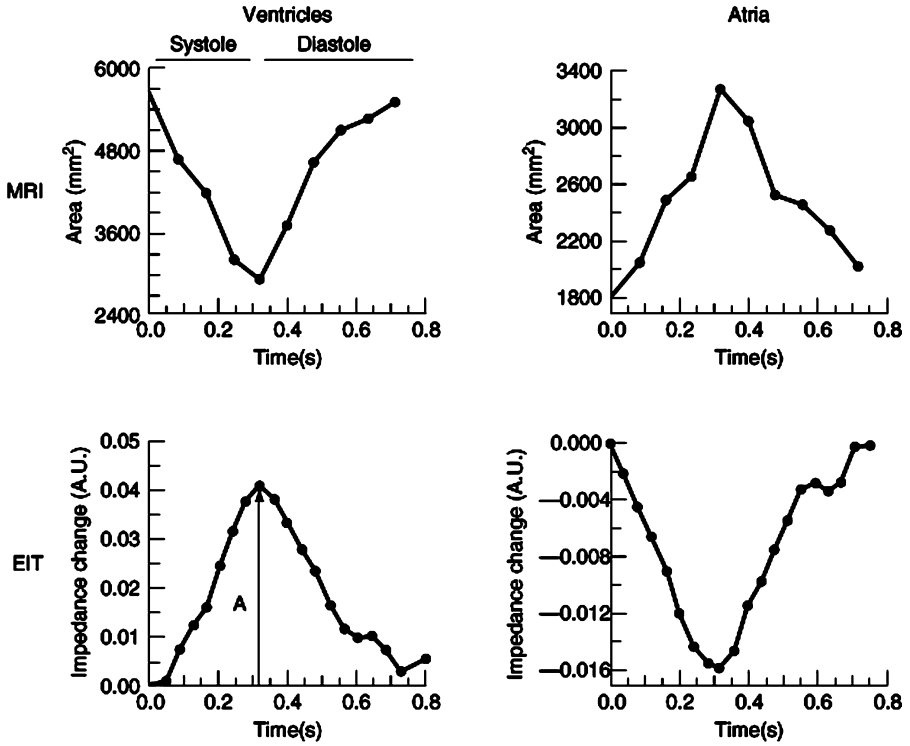

Figure 6. Variations of left ventricular and atrial cross-sectional area in the magnetic resonance imaging (MRI) and the electrical impedance tomography (EIT) images made with the person in the supine position. (From Ref. 29, with permission.)

the day, cardiac problems, and hypertension. Snoring may lead to soft tissue damage, notably an edematous uvula. Sudden death due to sleep apnea is often related to comorbidity and is probably rare. The standard measurement in sleep apnea includes the polysomnography repertoire, which consists of recording ECG, electroencephalogram, electro-oculogram, electromyogram of the legs, measurement of oral airflow with the use of thermistors, esophageal pressure, recording of snoring sound intensity, and plethysmography to estimate movements of chest and abdomen, besides the determination of arterial oxygen saturation. Typical costs associated with these studies amount up to $1000 or even more. Treatment may include simple advice to lose weight and avoid taking alcoholic drinks or sleeping pills but may also consist of various surgical procedures or continuous positive airway pressure (CPAP).

Apnea monitoring is based on either the measurement of bioelectric impedance or on estimation of biopneumatic impedance. Obviously, the time pattern of respiration is of primary interest for monitoring in these cases, and quantitative volume changes are of less importance, thus permitting simple instrumentation. The bioelectric technique is virtually identical to the ICG method, but in the present case the periodic circulatory components are regarded as perturbations superimposed on the slower respiratory signal. This signal is recorded with electrodes in the midaxillary line, and it may typically amount to 1 Ω per liter lung volume change, increasing with inspiration. The cardiac contribution (usually about 20% of the total amplitude) can (at least in humans) be determined during voluntary temporary respiratory interruption. Movement of the body causes artifacts, which may induce impedance changes in excess of the signal under investigation. An area that may be explored in this field concerns measurement of the motion of the diaphragm: with well-positioned electrodes the motion of this good conductor is easily assessed, while the changes of the signal are clearly related to respiration.

TISSUE CHARACTERIZATION: TWO- AND FOUR-ELECTRODE SYSTEMS

Electrical parameters of biological material are found to correlate with tissue structure and their (patho-)physiological changes (48). As mentioned before, muscle and blood exhibit different conductivities depending on the frequency employed. Muscle tissue is more conductive at frequencies above 12 kHz when the current is applied in a direction normal to the fiber orientation (37). Either two- or four-electrode systems have been employed for this type of tissue characterization, in combination with a bridge technique or phase sensitive detector method (using a lock-in amplifier). Although simple in design, the two-electrode system is less useful because of the presence of a charge distribution at the interface of the metal electrode and the tissue. However, this undesired effect of electrode polarization can be eliminated by the use of the four-electrode technique, with separate pairs of electrodes for current injection and for sensing the resulting potential difference (49). To calculate resistivity of a particular sample volume, it is necessary to select an electrical volume conductor model that sufficiently describes the geometry and conductive properties of the medium under study. Often, the medium can be approximated as an infinite or semi-infinite structure, or as a thin layer bounded by air on both sides.

Anisotropy is an important but complex aspect of the dielectric properties of tissue (26–51), which may be accommodated by considering a multilayered volume conductor model. (52) determined local anisotropic resistivity of canine epicardial tissue (i.e., the outer muscle layer of the ventricular wall) *in vivo* in two orthogonal directions, with special attention to sample volume. The effective sample volume for a simple homogeneous isotropic medium primarily depends on the distance between the current electrodes, but for real anisotropic media these researchers found that in addition both longitudinal and transverse resistivity (Ω·cm) varied not only during the cardiac cycle but also depended on the driving frequency studied (which was between 5 kHz and 60 kHz). Finally, it must be emphasized that electrode construction affects accuracy (51).

IMPEDANCE TOMOGRAPHY

This is a technically advanced approach whereby the imaging of an object is realized from measurements in multiple directions. Usually, 16 to 32 electrodes are placed equidistantly in a plane around the patients. This yields anatomical slices or sections, which can be viewed from various angles. Reasonably good soft tissue contrast can be achieved by impedance imaging, because of the different electrical resistivities of the various tissues. Impedance images are inferior to alternative techniques such as computed tomography and magnetic resonance imaging (MRI). Due to the three-dimensional spread of current into the object, the slice thickness cannot be confined to 1 mm or 2 mm. The strength of impedance tomography, however, resides in its functional imaging capabilities. Functional imaging is possible if variations in tissue resistivity are associated with particular physiological events. The first *in vivo* impedance tomography images were produced in 1983 at the University of Sheffield, and the theoretical background as well as illustration have been summarized by (53). A newer example has already been mentioned, when the right atrium was selected as the region of interest, and compared with results from MRI. (21) noninvasively assessed right ventricular diastolic function in patients with chronic obstructive pulmonary disease and in controls by means of region of interest analysis applied to electrical impedance tomography. Comparison with MRI data showed a correlation of $r = 0.78$ ($n = 15$), while pulmonary artery pressure (measured by right-sided heart catheterization) yielded an exponential relationship with $r = 0.83$ ($p < .001$). The same authors (29) also improved cardiac imaging in electrical impedance tomography by means of a new electrode configuration, whereby the traditional transversal positioning at the level of the fourth intercostal space on the anterior side was replaced by attachment at an oblique plane at the level of the ictus cordis anteriorly and 10 cm higher posteriorly. Comparison with MRI findings gave good results (Fig. 6), while the reproducibility coefficient was 0.98 at rest and 0.85 during exercise.

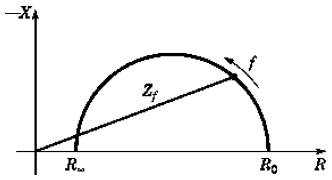

Figure 7. Cole–Cole diagram for an impedance with a single time constant.

IMPEDANCE SPECTROSCOPY

As stated before tissues can be considered as composites of cells surrounded by extracellular fluids. Each cell has a cell membrane that encloses intracellular fluid and consists of a thin layer of lipoproteins (≈6 nm). At low frequencies (<10 kHz) the cell membranes have relative high resistances, and the current is conducted mainly by the extracellular fluid. At high frequencies the membrane capacity causes a decrease of membrane impedance so that the current flows through the cells. The electrical behavior of a cell can be modelled by a membrane capacitance parallel to a membrane resistance in series with pure passive resistive elements, representing extra- and intracellular fluids. Coupling of several such modelled cells results in 2- or even 3-dimensional models of tissue. For the measurement of the frequency dependency of tissues two methods are often used, a resistance R in series with a reactance X or a conductance G parallel to a capacitance C. The complex impedance Z in the first approach is given by $Z = R + jX$. In the second approach the admittance Y is given by $Y = G + j\omega C$. As the complex impedance is the reciprocal of the admittance the following relations hold $R = G/(G^2 + \omega^2 C^2)$ and $X = -\omega C/(G^2 + \omega^2 C^2)$.

The complex series impedance $(R + jX)$ can be visualized in a diagram, in which the real component R is plotted versus the imaginary component X. In the literature this plot is often called the Cole–Cole diagram (54). In Fig. 7 the Cole–Cole diagram is given for a single time constant, where the impedance as a function of frequency is given by

$$Z = R_\infty + \frac{R_0 - R_\infty}{1 + j\omega\tau}$$

with R_0 the resistance at $f = \infty$ Hz and $\tau = CR$ a time constant.

The diagram is a semicircle with a radius (r), $r = (R_0 - R_\infty)/2$ and points of intersection with the horizontal axis R_0 and R_∞.

Although the complex series impedance of tissue is often plotted as a Cole–Cole diagram, in practice most tissues are best described with a semicircle with center slightly under the horizontal axis. Changes in tissue can be caused by changes in the amount of extra- and intracellular fluid, changes in tissue composition (e.g., tissue growth, ischemia, infarction, tumors, increase of adipose tissue) and can be measured and visualized in such plots (55, 56). This type of research is called impedance spectroscopy.

BIBLIOGRAPHY

1. B. C. Penney Theory and cardiac applications of electrical impedance measurements, *CRC Crit. Rev. Biomed. Eng.*, **13**: 227–281, 1986.
2. J. J. Ackman A. Seitz, Methods of complex impedance measurements in biologic tissue, *CRC Crit. Rev. Biomed. Eng.*, **11**: 281–311, 1984.
3. K. R. Foster P. Schwan, Dielectric properties of tissues and biological materials: A critical review, *Crit. Rev. Biomed. Eng.*, **17**: 25–104, 1989.
4. L. A. Geddes L. E. Baker *Principles of Applied Biomedical Instrumentation*, 3rd ed., New York: Wiley, 1989.
5. H. P. Schwan Electrode arization impedance and measurements in biological materials, Ann. N.Y. Acad. Sci., **148**: 191–209, 1968.
6. Y. Kim P. H. Schimpf Electrical behavior of defibrillation and pacing electrodes, *Proc. IEEE*, **54**: 446–456, 1996.
7. H. D. Fuller Evaluation left ventricular function by impedance cardiography: A review, *Prog. Cardiovasc. Dis.*, **36**: 267–273, 1994.
8. E. Raaijmakers et al meta- analysis of published studies concerning the validity of thoracic impedance cardiography, *Crit. Care Med.*, **27**: 1203–1213, 1999.
9. H. H. Woltjer et, Prediction of pulmonary capillary wedge pressure and assessment of stroke volume by noninvasive impedance cardiography, *Am. Heart J.*, **134**: 450–455, 1997.
10. L. W. Heather A parison of cardiac output values by the impedance cardiograph and dye dilution techniques in cardiac patients, NASA CR. 10 **N70-10015**: 247–258, 1969.
11. R. P. Patterson L. Wang S. B. Raza Impedance cardiography using band and regional electrodes in supine, sitting, and during exercise, *IEEE Trans. Biomed. Eng.*, **38**: 393–400, 1991.
12. F. H. Bonjer Circulatieonderzoek door impedantiemeting (in Dutch), Thesis, University of Groningen, The Netherlands, 1950.
13. W. G. Kubicek, *et al.* Development and evaluation of an impedance cardiac output system, *Aerospace Med*, **37**: 1208–1212, 1966.
14. J. Nyboer *Electrical Impedance Plethysmography*, Springfield, IL: Charles C. Thomas, 1970.
15. A. K. Barros N. Ohnishi MSE behavior of biomedical event-related filters, *IEEE Trans. Biomed. Eng.*, **44**: 848–855, 1997.
16. D. W. Kim C. G. Song M. H. Lee, A new ensemble averaging technique in impedance cardiography for estimation of stroke volume during treadmill exercise, *Frontiers Med. Biol. Eng.*, **4**: 171–178, 1992.
17. E. Raaijmakers, *et al.* he influence of extracellular lung water on cadiac output measurements using thoracic impedance cardiography, *Physiol. Meas.*, **19**: 491–499, 1998.
18. E. Raaijmakers, *et al.* Estimation of non-cardiogenic pulmonary oedema using dual-frequency electrical impedance, *Med. Biol. Eng. Comp.*, **36**: 461–466, 1998.
19. E. Raaijmakers, *et al.* The inaccuracy of Kubicek's one-cylinder model in thoracic impedance cardiography, *IEEE Trans. Biomed. Eng.*, **44**: 70–76, 1997.
20. G. Metry, *et al.* Gender and age differences in transthoracic bioimpedance, *Acta Physiol. Scand.* **161**: 171–175, 1997.

21. A. Vonk Noordegraaf, *et al.* Noninvasive assessment of right ventricular diastolic function by electrical impedance tomography, *Chest*, **111**: 1222–1228, 1997.
22. P. E. Marik J Pendelton R. Smith, A comparison of hemodynamic parameters derived from transthoracic electrical bioimpedance with those parameters obtained by thermodilution and ventricular angiography, *Crit. Care Med.*, **25**: 1545–1550, 1997.
23. R. M. Heethaar, *et al.* Thoracic electrical bioimpedance: Suitable for monitoring stroke volume during pregnancy? *Eur. J. Obstet. Gynecol. Reprod. Biol.*, **58**: 183–190, 1995.
24. A. C. C van Oppen, *et al.* Use of cardiac index in pregnancy: Is it justified? *Am. J. Obstet. Gynecol.*, **173**: 923–928, 1995.
25. H. J. Burgess, *et al.* Sleep and circadian influences on cardiac autonomic nervous system activity, *Am. J. Physiol.*, **42**: H1761–H1768, 1997.
26. L. Wang R Paterson Multiple sources of the impedance cardiogram based on 3-D finite difference human thorax models, *IEEE Trans. Biomed. Eng.*, **42**: 141–148, 1995.
27. M. Qu *et al.* Motion artifact from spot and band electrodes during impedance cardiography, *IEEE Trans. Biomed. Eng.*, **33**: 1029–1036, 1986.
28. D. W. Kim Detection physiological events by impedance, *Yonsei Med. J.*, **30**: 1–11, 1989.
29. A. Vonk Noordegraaf, *et al.* Improvement of cardiac imaging in electrical impedance tomography by means of a new electrode configuration, *Physiol. Meas.*, **17**: 179–188, 1996.
30. R. F. Rushmer, *et al.* Intracardiac impedance plethysmography, *Am. J. Physiol.*, **174**: 171, 1953.
31. M. E. Valentinuzzi J. C. Spinelli Intracardiac measurements with the impedance technique, *IEEE Eng. Med. Biol. Mag.*, **8** (1): 27–34, 1989.
32. G. Murand J Baan Computation of the input impedance of a catheter for cardiac volumetry, *IEEE Trans. Biomed. Eng.*, **31**: 448–453, 1984.
33. J. Baan *et al.* Continuous stroke volume and cardiac output from intraventricular dimensions obtained with impedance catheter, *Cardiovasc. Res.*, **15**: 328–334, 1981.
34. J. Baan *et al.* Ventricular volume measured from intracardiac dimensions with impedance catheter: Theoretical and experimental aspects, in T. Kenner, R. Busse, and H. Hingkefer-Szalkay (eds.), *Cardiovascular System Dynamics*, New York: Plenum, 1982, pp. 569–579.
35. P. L. M. Kerkhof End-systolic volume and the evaluation of cardiac pump function, Thesis, Leiden University, 1981.
36. T. J. Gawne K Gray R. E. Goldstein Estimating left ventricular offset volume using dual-frequency conductance catheters, *J. Appl. Physiol.*, **63**: 872–876, 1987.
37. E. Zheng S. Shao J. G. Webster Impedance of skeletal muscle from 1 Hz to 1 MHz, *IEEE Trans. Biomed. Eng.*, **31**: 477–481, 1984.
38. R. S. Szwarc, *et al.* Conductance catheter measurement of left ventricular volume in the intact dog: Parallel conductance is independent of left ventricular size, *Cardiovasc. Res.*, **28**: 252–258, 1994.
39. R. J. M. Klautz, *et al.* Interaction between afterload and contractility in the newborn heart, *J. Am. Coll. Cardiol.*, **25**: 1428–1435, 1995.
40. P. Schiereck, *et al.* Direct recording of EDP-EDV relationship in isolated rat left ventricle: Effect of diastolic crossbridge formation, *Cardiovasc. Res.*, **28**: 715–719, 1994.
41. H. Ito, *et al.* Left ventricular volumetric conductance catheter for rats, *Am. J. Physiol.*, **270**: H1509–H1514, 1996.
42. J. Vogel Measurement of diac output in small laboratory animals using recordings of blood conductivity, *Am. J. Physiol.*, **273**: H2520–H2527, 1997.
43. P. L. M. Kerkhof Combination of Millar and conductance catheter for the estimation of left ventricular function in the equine heart, Proc. 21st Int. Conf., *IEEE Eng. Med. Biol. Soc.*, 1999.
44. J. E. Axenborg B. Olsson, An electrical impedance method for measurement of aortic cross-sectional areas, *Proc. XII Int. Conf. Med. Biol. Eng.*, Jerusalem, 1979, P. 48.1.
45. L. Kornet Extension and imrovements of the electrical conductance method, Thesis, Erasmus University, Rotterdam, The Netherlands, 1996.
46. L. E. Baker Applications the impedance technique to the respiratory system, *IEEE Eng. Med. Biol. Mag.*, **8** (1): 50–52, 1989.
47. P. L. M. Kerkhof Beat-to-beat analysis of high-fidelity signals obtained from the left ventricle and aorta in chronically instrumented dogs, *Automedica*, **7**: 83–90, 1986.
48. I. Giaever C. R. Keese A morphological biosensor for mammalian cells, *Nature*, **366**: 591–592, 1993.
49. R. Plonsey R. C. Barr The four-electrode resistivity technique as applied to cardiac muscle, *IEEE Trans. Biomed. Eng.*, **29**: 541–546, 1982.
50. B. R. Epstein K. R. Foster Anisotropy in the dielectric properties of skeletal muscle, *Med. Biol. Eng. Comput.*, **21**: 51–55, 1983.
51. Y. Wang, *et al.* Geometric effects on resistivity measurements with four electrode probes in isotropic and anisotropic tissues, *IEEE Trans. Biomed. Eng.*, **45**: 877–884, 1998.
52. P. Steendijk *et al.* The four-electrode resistivity technique in anisotropic media: Theoretical analysis and application to myocardial tissue in vivo, *IEEE Trans. Biomed. Eng.*, **40**: 1138–1148, 1993.
53. B. M. Eyuboglu B. H. Brown D. C. Barber In vivo imaging of cardiac related impedance changes, *IEEE Eng. Med. Biol. Mag.*, **8** (1): 39–45, 1989.
54. K. S. Cole *Membranes, Ions and Impulses, Ions and Impulses*, Berkeley: Univ. California Press, 1972.
55. M. Gheorghiu E. Gersing E. Gheoghiu Quantitative analysis of impedance spectra of organs during ischemia, *Proc. 10th Int. Conf. Electrical Bio-impedance*, 1998, pp. 73–76.
56. H. Schäfer, *et al.* Dielectric properties of skeletal muscle during ischemia in the frequency range from 50 to 200 Hz, *Proc. 10th Int. Conf. Electrical Bio-impedance*, 1998, pp. 77–80.

Further reading:

S. Grimnes & Ø. G. Martinsen:"Bioimpedance and Bioelectricity Basics", Academic Press (2000). ISBN 0-12-303260-1

D. S. Holder:"Electrical Impedance Tomography".Institute of Physics Publishing (2005). ISBN 0-7503-0952-0

Relevant URL's:

Oslo Bioimpedance Group: http://www.fys.uio.no/elg/bioimp/

Thoracic electrical bioimpedance: http://www.aetna.com/cpb/data/CPBA0472.html

Clinical applications and guidelines: http://www.regence.com/trgmedpol/medicine/med33.html

Animation:

Thorax cross section: http://www.cplire.ru/html/tomo/eitimage.html

Software for impedance measurement:

http://www.elin.ttu.ee/BME-Wg/R&D/BImpMeas/SOFTWARE.HTM

http://www.sciencemag.org/cgi/reprint/224/4655/1355.pdf

PETER L. M. KERKHOF
ROBERT M. HEETHAAR
Vrije Universiteit Medical Center, Amsterdam, the Netherlands
Vrije University, Amsterdam, the Netherlands